Cranney, M., Cundall, R. B., Jones, G. R., Richards, J. T., & Thomas, E. W. (1983) *Biochim. Biophys. Acta 735*, 418–425.
Eftink, M. R., & Ghiron, C. A. (1976) *J. Phys. Chem. 80*, 486–493.
Gabbay, E. J., Grier, D., Fingerle, R. E., Reimer, R., Levy, R., Pearce, S. W., & Wilson, W. D. (1976) *Biochemistry 15*, 2062–2070.
Goormaghtigh, E., Chatelain, P., Caspers, J., & Ruysschaert, J. M. (1980) *Biochim. Biophys. Acta 597*, 1–14.
Jain, M. K. (1980) in *Introduction to Biological Membranes* (Jain, M. K., & Wagner, R. C., Eds.) Wiley, New York.
Jendrasiak, G. L. (1972) *Chem. Phys. Lipids 9*, 133–146.
Karczmar, G. S., & Tritton, T. R. (1979) *Biochim. Biophys. Acta 557*, 306–319.
Kersten, W., Kersten, H., & Szybalski, W. (1966) *Biochemistry 5*, 236–244.
Lakowicz, J. R. (1983) in *Principles of Fluorescence Spectroscopy* (Lakowicz, J. R., Ed.) Plenum Press, New York.
Lakowicz, J. R., & Knutson, J. R. (1980) *Biochemistry 19*, 905–911.
Lakowicz, J. R., Prendergast, F. G., & Hogen, D. (1979a) *Biochemistry 18*, 508–519.
Lakowicz, J. R., Prendergast, F. G., & Hogen, D. (1979b) *Biochemistry 18*, 520–527.
Menozzi, M., Valentini, L., Vannini, E., & Arcamone, F. (1984) *J. Pharm. Sci. 73*, 766–770.
Pigram, W. J., Fuller, W., & Hamilton, L. D. (1972) *Nature (London), New Biol. 235*, 17–19.
Record, M. T., Jr., Anderson, C. F., & Lohman, T. M. (1978) *Q. Rev. Biophys. 11*, 103–178.
Siegfried, J. M., Burke, T. G., & Tritton, T. R. (1985) *Biochem. Pharmacol. 34*, 593–598.
Spencer, R. D., & Weber, G. (1969) *Ann. N.Y. Acad. Sci. 158*, 361–376.
Suurkuusk, J., Lentz, B. R., Barenholz, Y., Biltonen, R. L., & Thompson, T. E. (1976) *Biochemistry 15*, 1393–1401.
Tritton, T. R., & Hickman, J. A. (1985) in *Experimental and Clinical Progress in Cancer Chemotherapy* (Muggia, F. M., Ed.) pp 81–131, Martinus Nijhoff, Boston, MA.
Tritton, T. R., Murphree, S. A., & Sartorelli, A. C. (1978) *Biochem. Biophys. Res. Commun. 84*, 802–808.

Long-Range Lipid–Protein Interactions. Evidence from Time-Resolved Fluorescence Depolarization and Energy-Transfer Experiments with Bacteriorhodopsin–Dimyristoylphosphatidylcholine Vesicles†

Mike Rehorek,‡ Norbert A. Dencher,§ and Maarten P. Heyn*,§

Biophysics Group, Department of Physics, Freie Universität Berlin, Arnimallee 14, D-1000 Berlin 33, West Germany, and Department of Biophysical Chemistry, Biocenter of the University of Basel, CH-4056 Basel, Switzerland

Received August 8, 1984; Revised Manuscript Received April 15, 1985

ABSTRACT: The effect of monomeric bacteriorhodopsin on the lipid order and dynamics in dimyristoylphosphatidylcholine (DMPC) vesicles was monitored as a function of the protein to lipid ratio by time-dependent fluorescence anisotropy measurements with diphenylhexatriene (DPH). Energy transfer from the donor DPH to the acceptor retinal of bacteriorhodopsin was used as a spectroscopic ruler to estimate the range of the protein-induced perturbation of the lipid phase. The Förster distance for this donor–acceptor pair is approximately 45 Å. Since the effective radius of bacteriorhodopsin is about 17 Å, the labels within a neighborhood of radius R_0 around bacteriorhodopsin are strongly quenched and make a negligible contribution to the end value of the fluorescence anisotropy, from which the order parameter is calculated. Instead, the order parameter is mainly determined by the labels which are more than the Förster distance away from the retinal and which are consequently in the bulk lipid phase. The observed linear increase in order parameter from 0.29 for pure DMPC to 0.62 for a molar bacteriorhodopsin to DMPC ratio of 1/52 thus indicates that the order of the bulk lipids is increased by the interaction with bacteriorhodopsin and that the range of this perturbation is larger than 45 Å. In the absence of the acceptor retinal, no energy transfer occurs, and both bulk and boundary lipids are weighted equally in the determination of the order parameter. Only a very small change in the order parameter is observed upon removal of the acceptor, suggesting that bacteriorhodopsin affects the order of all the lipids in roughly the same way. The rotational diffusion constant of DPH determined from the initial slope of the anisotropy decay is independent of the surface concentration of bacteriorhodopsin and of the presence of the acceptor retinal. The viscosity calculated from the rotational diffusion constant is approximately 0.1 P at 35 °C and is an order of magnitude smaller than that determined previously from the rotational diffusion of bacteriorhodopsin. A comparison of the viscosities determined from the steady-state and time-resolved fluorescence anisotropy of DPH shows that the first method overestimates the viscosity by as much as a factor of 10.

When proteins are incorporated in lipid bilayers, the physical properties of the lipids are usually changed. The order and dynamics of the hydrocarbon chains will be affected, and the phase transition will be broadened and occasionally shifted. The considerable amount of work which has been done to date to characterize these aspects of lipid–protein interactions was recently reviewed (Jost & Griffith, 1983). One of the central questions remains unanswered, however. Is the perturbation

† This work was supported by the Schweizerische Nationalfonds (Grant 3.623.80) and by the Deutsche Forschungsgemeinschaft.
‡ Biocenter of the University of Basel.
§ Freie Universität Berlin.

0006-2960/85/0424-5980$01.50/0

caused by the proteins restricted to a small neighborhood around them (boundary lipids), or do these changes have a long-range character and extend to most or all of the lipids (bulk lipids)? In other words, what is the range of this interaction? Fluorescence energy-transfer methods are quite useful to study this question, since during the lifetime of the excited state (usually not longer than 10 ns) no significant lateral diffusion of the label occurs. The fluorescence signal is thus an ensemble average over labels which are in various fixed environments. With slower methods, a single label will sample both the boundary and bulk environments. A further advantage of fluorescence is that by use of an appropriate acceptor within the protein, the fluorescence from lipids or probes in the immediate neighborhood of the protein may be entirely quenched by energy transfer. When the Förster distance of the donor–acceptor pair is much larger than the protein radius, only the bulk lipids will contribute to the end value of the fluorescence anisotropy, which in turn determines the order parameter. An increase of the order parameter when a protein with such an acceptor is incorporated is thus clear evidence for the long-range character of the lipid–protein interaction. By repeating the experiment in the absence of the acceptor, the contribution of the previously masked boundary lipids may be determined. An important variable to change in such experiments is the protein to lipid ratio, which enables one to vary the relative contribution of bulk and boundary lipids.

These ideas were tested with a vesicle system consisting of dimyristoylphosphatidylcholine (DMPC)[1] and bacteriorhodopsin (BR) at various protein to lipid ratios. This system has been extensively characterized (Cherry et al., 1978; Heyn et al., 1981a,b; Heyn & Dencher, 1982; Dencher et al., 1983). Above T_c, the BR molecules are in the monomeric state. The protein to lipid ratio can be varied over a wide range. As a fluorescence probe, 1,6-diphenyl-1,3,5-hexatriene (DPH) was used. Previous steady-state fluorescence depolarization measurements with this probe showed that an increase in the protein to lipid ratio leads to a large increase in the fluorescence anisotropy (Heyn, 1979; Heyn et al., 1981a). The present time-resolved fluorescence anisotropy experiments were designed to determine whether this increase is due to an increase in lipid order, to an increase in lipid viscosity, or to a combination of both effects. The previously observed changes in steady-state anisotropy were so large, however, that a significant increase in order seemed quite likely (Heyn, 1979; Heyn et al., 1981a). Energy transfer occurs with high efficiency from DPH to the acceptor retinal in BR, with a Förster distance of about 45 Å (Rehorek et al., 1983; Heyn et al., 1983). By irradiation with visible light, the acceptors can be easily destroyed. From these energy-transfer experiments, it was concluded that the retinal chromophore of BR is located in the interior of the protein (Rehorek et al., 1983; Heyn et al., 1983). This result was recently confirmed by neutron diffraction experiments with deuterated retinal (Seiff et al., 1985). The lifetime of DPH is much reduced in the presence of energy transfer, leading to an increase in steady-state fluorescence anisotropy. Repeating the steady-state experiments in the absence of the acceptor showed, however, that the major part of the protein-induced increase in steady-state anisotropy is due to lipid–protein interactions rather than to energy transfer. The BR–DMPC vesicle system is thus quite appropriate for carrying out the strategy described above. Vesicles of various BR to DMPC ratios were incubated with DPH. The time-resolved fluorescence depolarization was measured in both the presence and absence of the acceptor retinal and interpreted in terms of an order parameter and a rotational diffusion constant. In this way, systematic data were collected concerning the change in order parameter and membrane viscosity as a function of the BR to DMPC ratio. Whereas the order parameter shows a large increase with increasing protein to lipid ratio, the membrane viscosity at 35 °C is almost independent of this ratio. The previously observed increase in steady-state fluorescence anisotropy is thus due to a protein-induced increase in lipid order. The energy-transfer experiments moreover allow an estimate of the range of the lipid–protein interactions. In contrast to a recent calculation of 15 Å (Jähnig, 1981), it is concluded that the range is larger than the Förster distance of 45 Å, implying a long-range interaction affecting most of the lipids.

Materials and Methods

Preparation of BR–DMPC Vesicles. The DMPC vesicles containing BR at various BR to DMPC ratios were prepared and characterized as described in detail elsewhere (Cherry et al., 1978; Heyn et al., 1981a,b; Heyn & Dencher, 1982). The molar BR/DMPC ratios (see also Table I) were 0 (vesicles 1), 1/393 (vesicles 2), 1/185 (vesicles 3), 1/174 (vesicles 4), 1/115 (vesicles 5), 1/97 (vesicles 6), and 1/52 (vesicles 7).

Removal of the Chromophore. To test the effect of energy transfer from DPH to the chromophore, retinal was destroyed by illuminating the samples with a 300-W xenon lamp ($\lambda > 320$ nm) (Rehorek et al., 1983).

Fluorescence Depolarization Measurements. Steady-state fluorescence depolarization measurements were performed on a Schoeffel fluorometer as described previously (Heyn et al., 1981a). DPH was incorporated in a molar DPH/DMPC ratio of 1/250. At this level of label incorporation, the phase transition curve was not affected (Heyn et al., 1981b).

Time-dependent fluorescence depolarization measurements were carried out on a single-photon counting apparatus as described elsewhere (Rehorek et al., 1983). The pulse width was 1.3–1.5 ns FWHM. The lamp was operated at a pulse frequency of 30 or 50 kHz. The excitation and emission light was passed through Glan prism polarizers (B. Halle, Optische Werkstätten, West Berlin). To average lamp instabilities, and to avoid lamp frequency fluctuations (<0.8%), the analyzer was rotated every 5×10^6 counts in the start channel (≈100 s). The excitation profile was measured before and after the anisotropy decay measurement, and the sum of the two pulses was used to analyze the data. The perpendicular component was corrected for differences in the sensitivity of the optical components (Badea & Brand, 1979). The so-called G factor was determined several times before and after the anisotropy decay measurement for each sample, under the same conditions as during the experiment, except that the polarizer was set to horizontally polarized excitation. The G factor was then calculated from the ratio of the total number of counts after the time to amplitude converter for vertically and horizontally polarized emission.

Data Analysis. The data were analyzed on a DEC LSI 11/23 minicomputer interfaced to the multichannel analyzer using a Marquardt nonlinear least-squares algorithm (Bevington, 1969; Grinvald & Steinberg, 1974; Grinvald, 1976) based on a model for the anisotropy decays described by Wahl (1979). In the first part of the computer program, the convolution integral (*) of the excitation function, $L(t)$, with a

[1] Abbreviations: BR, bacteriorhodopsin; DPH, 1,6-diphenyl-1,3,5-hexatriene; T_c, midpoint temperature of the lipid gel to liquid-crystalline phase transition; FWHM, full width at half-maximum; DMPC, dimyristoylphosphatidylcholine; R_0, Förster radius.

sum of one to three exponentials was fitted to the experimental fluorescence decay curve:

$$S_{calcd}(t) = L(t)*f(t) \quad \text{with} \quad f(t) = \sum_i \alpha_i e^{-t/\tau_i} \quad (1)$$

$$S_{exptl}(t) = I_{\parallel}(t) + 2GI_{\perp}(t) \quad (2)$$

$S_{calcd}(t)$, the parameters α_i and τ_i, and the time shift between $L(t)$ and $S_{exptl}(t)$ (Grinvald, 1976) were stored in the computer memory for later use. In the second part of the program, the convolution of $L(t)$ with the product of $f(t)$ and $r(t)$, divided by $S_{calcd}(t)$, was fitted to $r_{exptl}(t)$, with the parameters α_i and τ_i and the time shift kept constant:

$$r_{calcd}(t) = L(t)*[f(t)r(t)]/S_{calcd}(t) \quad (3)$$

$$r_{exptl}(t) = [I_{\parallel}(t) - GI_{\perp}(t)]/S_{exptl}(t) \quad (4)$$

In the computer program, two models for $r(t)$ were implemented:

model 1

$$r(t) = r_\infty + \sum_{j=1}^{N} r_j e^{-t/\phi_j} \quad N = 1 \text{ or } 2 \quad (5)$$

with

$$r_0 = r_\infty + \sum_{j=1}^{N} r_j \quad (6)$$

or

model 2

$$r(t) = r_\infty + (r_0 - r_\infty)[Re^{-t/\phi_1} + (1 - R)e^{-t/\phi_2}] \quad (7)$$

with

$$r_0 = \text{constant (e.g., 0.4)} \quad \text{and} \quad R = r_1/(r_0 - r_\infty) \quad (8)$$

For the analysis of our anisotropy decay data, it was always necessary to use a sum of two exponentials plus a constant term (r_∞). The correct determination of r_0 from the sum of the preexponentials (eq 6) is very difficult, especially if ϕ_1 is short. It strongly depends on the channel number from where the fit was started. The large errors in the amplitude of the short component (0.2–0.5 ns) determine the errors in r_0. Whenever r_0 was fitted, the theoretical maximum value of 0.4 was within the error bars. Therefore, $r_0 = 0.4$ was chosen empirically for the analysis of all the decay curves (Kawato et al., 1977: $r_0 = 0.395$), and the ratio of the two amplitudes was fitted (model 2). The fit of $r(t)$ was usually started at the channel number where the rising edge of the lamp pulse was approximately at 50% of its maximal value. The weights for the calculation of the reduced χ^2, χ_ν^2, for $S(t)$ and $r(t)$ were calculated from $\sigma_{\parallel}^2 = I_{\parallel}$ and $\sigma_{\perp}^2 = I_{\perp}$ by using the error propagation law (Wahl, 1979).

The steady-state anisotropy, $\bar{r}$, measured at the Schoeffel fluorometer was compared for each sample with the corresponding steady-state anisotropy, $\langle r(t)\rangle$, calculated from the parameters of the anisotropy decay:

$$\langle r(t)\rangle = \frac{\int_0^\infty r(t)f(t)\,dt}{\int_0^\infty f(t)\,dt} = r_\infty + \frac{r_0 - r_\infty}{\sum_i \alpha_i\tau_i}\left[R\phi_1\sum_i \frac{\alpha_i\tau_i}{\phi_1 + \tau_i} + (1 - R)\phi_2\sum_i \frac{\alpha_i\tau_i}{\phi_2 + \tau_i}\right] \quad (9)$$

Calculation of the Order Parameter and the Membrane Viscosity. The order parameter S was calculated according to (Heyn, 1979; Jähnig, 1979)

$$S = (r_\infty/r_0)^{1/2} \quad \text{with} \quad r_0 = 0.4 \quad (10)$$

The rotational diffusion constant was calculated in two ways: (1) from the theory of the "cone model" (Kinosita et al., 1977; Lipari & Szabo, 1980); and (2) from the initial slope of the anisotropy decay, which is model independent (Kinosita et al., 1977, 1982).

The single-exponential approximation of the cone model is correct at $t = 0$ (r_0) and $t = \infty$ (r_∞) and has the correct area under the time-dependent part of the decay curve (Kinosita et al., 1977; Lipari & Szabo, 1980). Since we always used a sum of two exponentials (plus r_∞) in the analysis of our anisotropy decay data, we had to choose an appropriate mean correlation time by integration:

$$\bar{\phi}_{int} = \int_0^\infty \frac{r(t) - r_\infty}{r_0 - r_\infty}\,dt = R\phi_1 + (1 - R)\phi_2 \quad (11)$$

In case 2, however, the appropriate mean correlation time was calculated from the derivative of $r(t)$ at time zero (Dale et al., 1977; Kinosita et al., 1977) and is therefore denoted by $\bar{\phi}_{der}$:

$$\bar{\phi}_{der} = -\left(\frac{\partial}{\partial t}\left[\frac{r(t) - r_\infty}{r_0 - r_\infty}\right]\right)_{t=0}^{-1} = \left(\frac{R}{\phi_1} + \frac{1 - R}{\phi_2}\right)^{-1} \quad (12)$$

The rotational diffusion coefficient for the wobbling in the cone was calculated by (Kinosita et al., 1977)

$$D_{int} = \langle\sigma\rangle/\bar{\phi}_{int} \quad (13)$$

where $\langle\sigma\rangle$ is a function of the cone angle, which can be calculated by using eq 24 of Lipari & Szabo (1980). The rotational diffusion coefficient was also calculated from the initial slope (Kinosita et al., 1982):

$$D_{der} = (1 - r_\infty/r_0)/6\bar{\phi}_{der} \quad (14)$$

The viscosity of the membrane bilayer was calculated according to (Kawato et al., 1977)

$$\eta = kT/6DV_e f \quad (15)$$

using either D_{int} or D_{der} for D. V_e and f denote the effective volume and shape factor of the probe, respectively, approximated by a prolate ellipsoid. The product $V_e f$ was calculated from anisotropy decay measurements of DPH in liquid paraffin, an isotropic medium of similar molecular nature as the hydrocarbon chains of the lipids (Cehelnik et al., 1974; Kawato et al., 1977). The viscosity of liquid paraffin (Merck Uvasol, Nr. 7161) was determined by using an Ubbelohde viscosimeter (Cannon 100).

Results

A comparison of the time integral of the anisotropy decay, $\langle r(t)\rangle$ (eq 9), with the corresponding steady-state anisotropy, $\bar{r}$, as shown in Figure 1, is a good test for the performance of the instrument, for the quality of the measurement, for the choice of the model for the data analysis, and for the internal consistency of the data. In spite of the different techniques and instruments, $\langle r(t)\rangle$ and $\bar{r}$ are in good agreement for all the vesicle suspensions. Whereas the data far below the phase transition temperature of DMPC [(■) unbleached; (□) bleached vesicles at 0.5 °C] are close together and independent of the BR/DMPC ratio, the data above T_c are varying over a wide range and are increasing with increasing BR/DMPC ratio, for both unbleached (●) and bleached (○) vesicles. The effect of BR on the phase transition of DMPC, as monitored by the steady-state fluorescence anisotropy of DPH ($\bar{r}$), is shown in Figure 2. The large increase in $\bar{r}$ above T_c in Figure 2A (unbleached vesicles) is less pronounced in the case of the

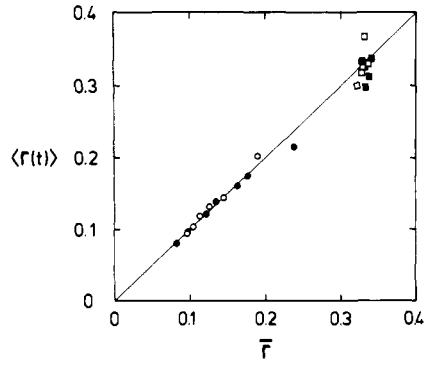

FIGURE 1: Comparison of the time average of the anisotropy decay, $\langle r(t) \rangle$, calculated according to eq 9, with the corresponding steady-state anisotropy, $\bar{r}$, at 0.5 (■, □) and 35 °C (●, ○). Open symbols: bleached vesicles.

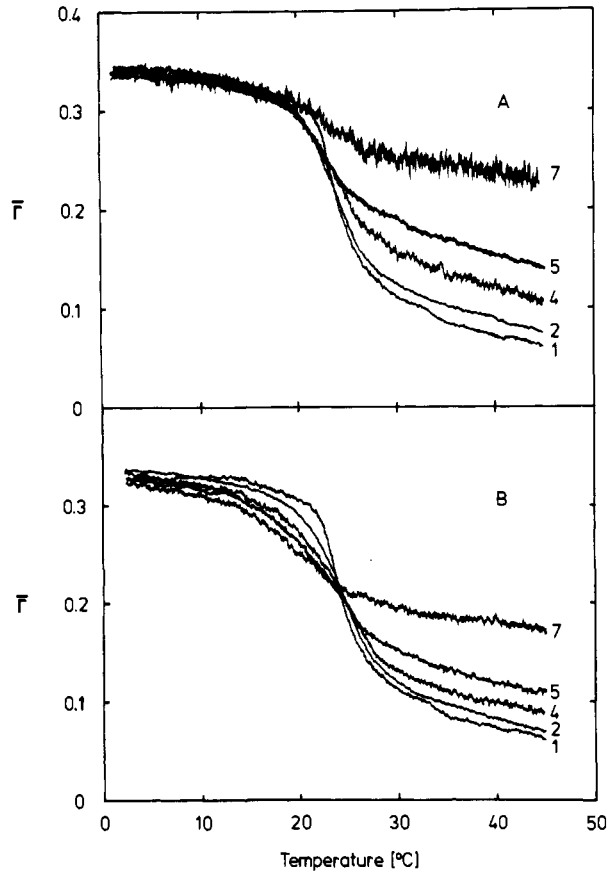

FIGURE 2: Steady-state anisotropy, $\bar{r}$, of DPH as a function of temperature for unbleached (A) and bleached (B) vesicles at various BR/DMPC ratios. The numbers correspond to the vesicle suspensions as defined under Materials and Methods and in Table I. For clarity, the curves for vesicles 3 and 6 have been omitted.

bleached vesicles (Figure 2B). The transition curves of the bleached vesicles are more symmetric, and, in contrast to the unbleached vesicles, BR leads to a clear decrease of $\bar{r}$ below T_c. This difference between unbleached and bleached vesicles can be explained by the strong fluorescence energy transfer from DPH to the chromophore retinal of BR (Rehorek et al., 1983). Above T_c, the shorter lifetime of DPH in the presence of the acceptor retinal leads to an increase of $\bar{r}$ and has to be separated from the increase, which arises from the proteins. Provided that bleaching does not alter the protein–lipid interactions, the increase in $\bar{r}$ above T_c in Figure 2B can be considered as the net effect of BR on the rotational correlation time and on the orientational order of the lipids (Heyn, 1979). On the basis of steady-state measurements alone, no distinction

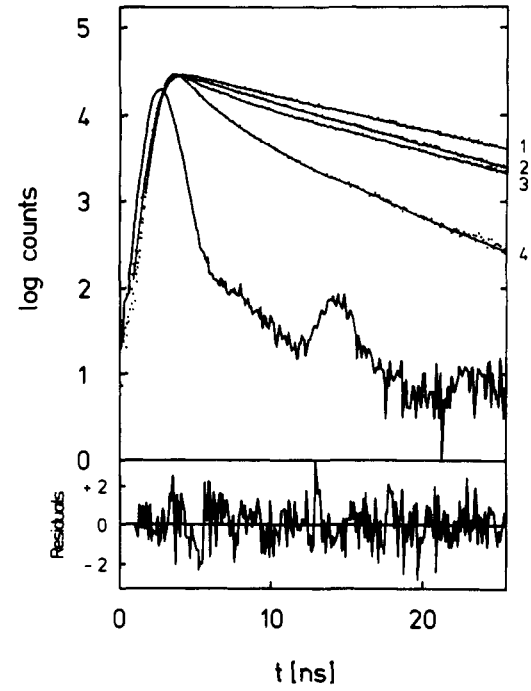

FIGURE 3: Lamp pulse and fluorescence decay curves (···) of DPH, calculated from the sum of the parallel and perpendicular components (eq 2), for vesicles 1 at 0.5 (curve 1) and 35 °C (curve 2) and for vesicles 5 at 0.5 (curve 3) and 35 °C (curve 4). Bottom: weighted residuals for curve 1.

between these effects is possible.

Evidence for energy transfer from DPH to retinal in the fluorescence decay of DPH is presented in Figure 3. Curves 1 and 2 show the single-exponential decays of DPH in pure DMPC vesicles (vesicles 1) at 0.5 and 35 °C, respectively. Due to energy transfer from DPH to the retinal of BR, the fluorescence decay is faster in the presence of BR and clearly nonexponential (curves 3 and 4), as is to be expected for a random two-dimensional distribution of donors and acceptors (Rehorek et al., 1983). The Förster radius, R_0, for this donor–acceptor pair was calculated in these vesicles to be in the range of 41–45 Å, depending on the order parameter S of DPH. Whereas above T_c the proteins are randomly distributed within the membrane plane (Cherry et al., 1978; Heyn et al., 1981a,b), below the phase transition of the lipids BR is aggregated in a hexagonal lattice. At 35 °C, the curvature of the decay (curve 4) is more pronounced than below T_c (curve 3), because the overlap of the energy-transfer regions, πR_0^2, around the proteins is much larger in the hexagonal lattice than in the monomeric state. Curves 1–3 of Figure 4 show the effect of BR, in the presence and absence of the acceptor retinal, on the anisotropy decay of DPH at 35 °C. The incorporation of proteins into DMPC vesicles leads to a marked increase in the end value of the decay, r_∞. From pure lipid vesicles (curve 1) to vesicles containing a large amount of BR (vesicles 7, 1/52, curve 3), an increase in r_∞ of 450% can be observed. Removing the chromophore (vesicles 7 bleached, curve 2) leads only to a small decrease in r_∞ of 30% with respect to the unbleached vesicles. For a comparison, the data at 0.5 °C are shown for DPH in pure DMPC vesicles (vesicles 1, curve 4). At this temperature, the decay curves of the vesicles containing BR were identical and therefore omitted in Figure 4. Note that the solid curves in Figure 4 represent the anisotropy decay curves, $r_{calcd}(t)$, after convolution with the lamp pulse according to eq 3. The bump in curve 3 around 15 ns is thus simply due to the corresponding bump in the lamp pulse (see Figure 3). This bump shows up only in curve 3,

Table I: Summary of Anisotropy Parameters at 35 °C

vesicles	BR/DMPC (mM/M) ratio	S	ϕ_{int} (ns)	ϕ_{der} (ns)	η_{int} (P)	η_{der} (P)	χ_ν^2
1	0	0.293 ± 0.004[b]	1.29 ± 0.07	0.44 ± 0.07	0.236 ± 0.014	0.122 ± 0.019	0.928
2	2.5 ● 0.3 (1/393)	0.320 ± 0.005	1.23 ± 0.08	0.46 ± 0.06	0.231 ± 0.015	0.130 ± 0.017	1.165
2b[a]		0.335 ± 0.004	1.36 ± 0.08	0.50 ± 0.06	0.259 ± 0.015	0.143 ± 0.017	0.917
3	5.4 ● 0.8 (1/185)	0.353 ± 0.005	1.21 ± 0.08	0.37 ± 0.06	0.235 ± 0.016	0.108 ± 0.016	1.040
3b		0.351 ± 0.005	1.58 ± 0.11	0.53 ± 0.05	0.307 ± 0.021	0.156 ± 0.015	0.997
4	5.8 ± 0.8 (1/174)	0.385 ± 0.007	1.35 ± 0.13	0.56 ± 0.06	0.274 ± 0.026	0.168 ± 0.019	1.079
4b		0.385 ± 0.005	1.56 ± 0.08	0.44 ± 0.05	0.316 ± 0.016	0.133 ± 0.014	0.996
5	8.7 ± 2.2 (1/115)	0.424 ± 0.006	1.16 ± 0.11	0.36 ± 0.06	0.247 ± 0.023	0.113 ± 0.018	0.999
5b		0.404 ± 0.004	1.97 ± 0.11	0.68 ± 0.06	0.407 ± 0.023	0.207 ± 0.018	0.954
6	10.3 ± 0.9 (1/97)	0.445 ± 0.009	1.39 ± 0.16	0.54 ± 0.05	0.305 ± 0.035	0.174 ± 0.017	0.982
6b		0.419 ± 0.006	1.86 ± 0.10	0.42 ± 0.05	0.392 ± 0.021	0.132 ± 0.017	1.002
7	19.3 ± 0.5 (1/52)	0.619 ± 0.007	0.98 ± 0.19	0.24 ± 0.05	0.296 ± 0.058	0.100 ± 0.020	1.081
7b		0.524 ± 0.008	2.76 ± 0.16	0.26 ± 0.06	0.689 ± 0.040	0.091 ± 0.021	1.031

[a] b = bleached. [b] Standard deviations, calculated from the error matrix and the error propagation law.

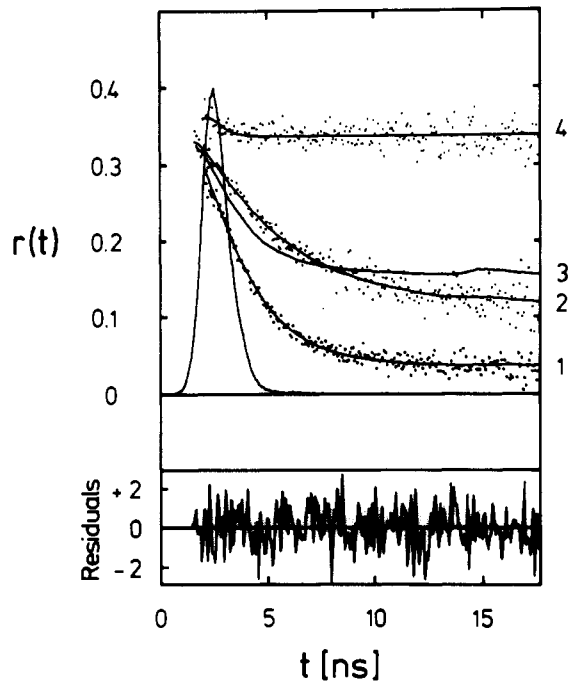

FIGURE 4: Experimental (···) and calculated (—) anisotropy decay curves for pure DMPC vesicles (vesicles 1) at 35 (curve 1) and 0.5 °C (curve 4) and for vesicles 7 (curve 3) and vesicles 7 bleached (curve 2) at 35 °C. For clarity, the data points of curve 3 have been omitted, but their weighted residuals are shown at the bottom. The bump in curve 3 near 15 ns arises from the after-pulse of the photomultiplier tube (see also Figure 3, lamp pulse). It is only observable for samples with a short lifetime. A normalized lamp pulse is shown on a linear scale.

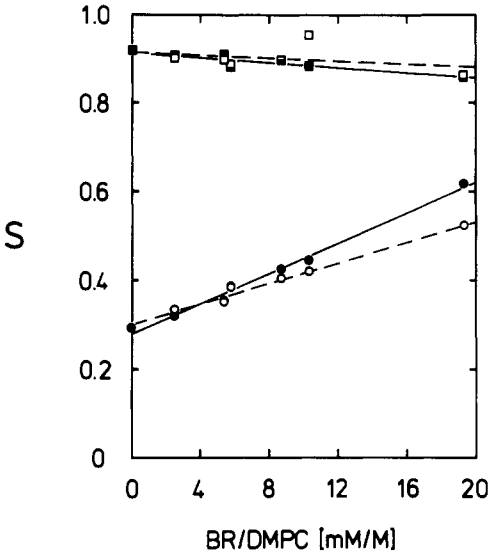

FIGURE 5: Order parameters of DPH incorporated in DMPC vesicles containing BR at various protein/lipid ratios at 0.5 (■, □) and 35 °C (●, ○). Open symbols: bleached vesicles. The straight lines correspond to least-squares fits to the data. Dashed lines: bleached vesicles. For vesicles 3 and 4 at 35 °C, the order parameters for the bleached and unbleached vesicles are the same.

since strong energy transfer leads to a very rapid decay of the fluorescence intensity in this case.

The parameters of the anisotropy decays can be converted into the model-independent order parameter S as calculated according to eq 10 (Heyn, 1979; Jähnig, 1979) and the microviscosity η (Dale et al., 1977; Kawato et al., 1977; Chen et al., 1977). The mean correlation times (eq 11 and 12), the order parameters (eq 10), and the viscosities (eq 15) are summarized in Table I as a function of the BR/DMPC ratio for the data obtained at 35 °C.

It was impossible to analyze the anisotropy decay curves with a single exponential plus a constant term, as proposed by Kinosita et al. (1977). In the case of pure lipid vesicles, for example, the χ_ν^2 value for such an analysis, with r_0 kept constant, was 3.55 (with $r_0 = 0.4$). If r_0 is calculated from the fitting parameters, $r_0 = r_1 + r_\infty$, it is always underestimated ($r_0 = 0.302$); the fit is somewhat better ($\chi_\nu^2 = 1.08$), but the residuals show systematic deviations. In both cases, the constant term, r_∞, is overestimated. A double-exponential analysis of the same data, with r_0 = constant = 0.4, yields a χ_ν^2 value of 0.928 ($\phi_1 = 0.23 \pm 0.03$ ns, $\phi_2 = 2.14 \pm 0.10$ ns, $R = 0.42 \pm 0.03$, and $r_\infty = 0.035 \pm 0.001$).

A comparison of the fits of the same data, using the lamp pulses as measured before (FWHM = 1.37 ± 0.01 ns) and after (1.36 ± 0.01 ns) the anisotropy decay measurement (about 2 h apart), showed that the parameters were identical within the error bars. The standard deviations of the parameters were calculated from the diagonal elements of the error matrix (Bevington, 1969). The relative errors of the parameters were usually of the order of ~15% (ϕ_1), ~7% (ϕ_2), ~6% (R), and ~3% (r_∞).

Figure 5 shows the order parameter S for all the samples at 0.5 (■, □) and 35 °C (●, ○) as a function of the BR/DMPC ratio. Far below the phase transition temperature of the lipids, the order parameter is very high (about 0.9) and almost independent of the BR/DMPC ratio, whereas above T_c, S increases by about a factor of 2 in going from the pure lipids to the highest protein to lipid ratio. The solid and the dashed lines represent straight line fits to the data. The difference in the slope between unbleached and bleached vesicles at 35 °C is significant at the 95% confidence level only if we include the point at the highest protein to lipid ratio. If we disregard that point, there is no statistically significant

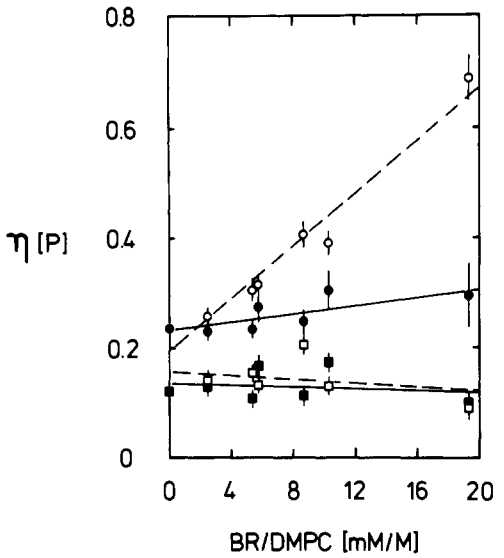

FIGURE 6: Microviscosities, η, calculated according to eq 15 by using D_{int} for the cone model [eq 11 and 13 (●, ○)] and D_{der} for the model-independent calculation [eq 12 and 14 (■, □)]. T = 35 °C. Open symbols: bleached vesicles. The straight lines correspond to least-squares fits of the data. Dashed lines: bleached vesicles.

difference in S in the bleached and unbleached states.

The interpretation of the correlation times in terms of rotational diffusion constants is more complicated. The correlation times of a rodlike probe, such as DPH, wobbling within the limits of an anisotropic environment, as, e.g., a membrane bilayer, depend on the extent of wobbling, i.e., on the order parameter S (Kinosita et al., 1977; Lipari & Szabo, 1980; Zannoni et al., 1983). A relationship between the correlation times and the rotational diffusion constant for the wobbling motion of a label within a cone, D_{int}, was derived by Kinosita et al. (1977). They showed that for such a model the anisotropy decay is an infinite sum of exponentials, in which the amplitudes depend on r_∞/r_0 and the correlation times on r_∞/r_0 and D_{int}. As an approximation, they proposed a single-exponential decay plus a constant term of the form

$$r(t)/r_0 = r_\infty/r_0 + (1 - r_\infty/r_0)e^{-D_{int}t/\langle\sigma\rangle} \qquad (16)$$

where $\langle\sigma\rangle$ is a function of r_∞/r_0. $\langle\sigma\rangle$ was derived from the requirement that the area under the time-dependent part of eq 16 be equal to the area under the time-dependent part of the exact decay curve. An analytical expression for $\langle\sigma\rangle$ was derived by Lipari & Szabo (1980).

The wobbling diffusion constant, D_{int}, was calculated according to eq 13 by using $\bar{\phi}_{int}$ (eq 11) instead of a single correlation time. $\bar{\phi}_{int}$ is clearly a better measure of the area under the decay curve than just a single ϕ.

An alternative way of getting the rotational diffusion constant is to calculate it from the initial slope of the anisotropy decay curve (eq 12 and 14) (Kinosita et al., 1977, 1982; Lipari & Szabo, 1980). In contrast to D_{int}, the calculation of D_{der} from the initial slope is model independent (Kinosita et al., 1982) and should therefore be preferred.

The microviscosities, η_{int} and η_{der} at 35 °C, calculated from eq 15 by using D_{int} and D_{der}, respectively, are plotted as a function of the BR/DMPC ratio in Figure 6. The product of the effective volume and shape factor, $V_e f$, in eq 15 was determined from anisotropy decay measurements of DPH in liquid paraffin of known viscosity. The viscosity of liquid paraffin at 30 °C was found to be 0.766 P. Using this value, we found $V_e f = 1.66 \times 10^{-22}$ cm^3, which was used for the calculations of η_{int} and η_{der}. This value may be compared with the following results taken from the literature: $(1.5–1.8) \times 10^{-22}$ cm^3 (Kawato et al., 1977), 1.5×10^{-22} cm^3 (Cehelnik et al., 1974), $(1.0–1.8) \times 10^{-22}$ cm^3 (Dale et al., 1977), and $(1.6–2.4) \times 10^{-22}$ cm^3 (Glatz, 1978). The average of these literature values (17 determinations) is $(1.63 \pm 0.34) \times 10^{-22}$ cm^3.

The closed and open circles in Figure 6 correspond to η_{int} calculated from the cone model (eq 11, 13, and 15) for unbleached and bleached vesicles. The squares correspond to η_{der} calculated, in the model-independent way, from the initial slope (eq 12, 14, and 15). The most striking feature in Figure 6 is that only the viscosities, η_{int}, from the cone model for the series of bleached vesicles (○) show a dependence on the BR/DMPC ratio. η_{int} for the unbleached vesicles (●) and also the viscosities (η_{der}) calculated from the initial slope for unbleached (■) and bleached vesicles (□) are within experimental accuracy independent of the protein content.

Discussion

Energy transfer is an excellent tool for studying lipid–protein interactions in this well-characterized system. As the rotational motion of a label can only be observed during its fluorescence lifetime, and as the lifetime of the label strongly depends on its distance to the acceptor retinal, the contribution of each label to the overall anisotropy depends on its distance from the protein. Assuming retinal to be in the center of BR (Rehorek et al., 1983) and taking a Förster radius of 45 Å, the lifetime of a DPH label at the surface of BR (17 Å away from the acceptor) is calculated to be about 0.03 ns. At 26 Å from the retinal, corresponding to the BR radius plus one layer of lipids, the lifetime is still only about 0.3 ns. The contribution of each label to the observed anisotropy is proportional to its fractional fluorescence intensity (Wahl, 1975):

$$r(t) = \sum_i r_i(t)S_i(t) / \sum_i S_i(t) \qquad (17)$$

In the presence of energy transfer, the labels within the lipid boundary region of the proteins thus make almost no contribution to the observed limiting anisotropy. The constant term in the anisotropy decay r_∞ and the order parameter S are determined by those labels which still fluoresce at 15–20 ns after excitation. The order parameter is thus determined by the labels with the longest lifetimes, i.e., the labels at distances further away from the retinal than R_0. Since the order parameter in the presence of energy transfer (unbleached vesicles) strongly depends on the BR/DMPC ratio, the conclusion is inescapable that the effect of BR is not restricted to "boundary" or "annular" lipids but has long-range character. In fact, its range must be at least of the order of R_0 (41–45 Å). The average distance between the centers of two BR molecules can be easily calculated from the BR/DMPC ratio and the surface areas of BR and DMPC (Rehorek et al., 1983). For vesicles 2 (BR/DMPC = 1/393), we calculate in this way an interprotein distance of about 126 Å. The lipids midway between two proteins are about 63 Å away from the center of each protein, corresponding to $1.43R_0$. For vesicles 7 with the highest protein to lipid ratio (1/52), the average interprotein distance is 56 Å, and the lipids midway between two proteins are only 28 Å ($0.63R_0$) away from the center. Over this large range of protein to lipid ratios, the change in S is to a good approximation linear (Figure 5). If the order parameter differs considerably between bulk and boundary lipids, a jump in S may be expected at the protein to lipid ratio where the labels which are most remote from the acceptors enter the boundary region. The data of Figure 5 are thus consistent with a homogeneous perturbation of the lipid phase. The best evidence in support of the notion that BR affects all of the lipids in the same way comes from the comparison of

Table II: Summary of Viscosity Values at 35 °C

vesicles	BR/DMPC (mM/M) ratio	r_∞	$\bar{r}$	η_{MV} (P)	η_{cor} (P)	η_{der} (P)	η_{BR} (P)
1	0	0.034	0.081	0.471	0.299	0.122	3.7 ± 1.3
2b[a]	2.5 ± 0.3	0.045	0.095	0.618	0.366	0.143	3.7 ± 1.3
3b	5.4 ± 0.8	0.049	0.103	0.721	0.430	0.156	3.7 ± 1.3
4b	5.8 ± 0.8	0.059	0.115	0.881	0.503	0.133	3.7 ± 1.3
5b	8.7 ± 2.2	0.065	0.128	1.077	0.633	0.207	3.7 ± 1.3
6b	10.3 ± 0.9	0.070	0.144	1.353	0.843	0.132	3.7 ± 1.3

[a] b = bleached; η_{MV} calculated according to eq 18 of Shinitzky & Barenholz (1978); η_{cor} calculated according to eq 11 of Heyn et al. (1981a); η_{BR} calculated from the rotational diffusion of BR (Cherry & Godfrey, 1981).

the data for the unbleached and bleached vesicles. Upon removal of the acceptor (bleached vesicles), the lifetime of DPH returns to its value of about 8 ns in the absence of energy transfer (Rehorek et al., 1983), and all labels in eq 16 are weighted in the same way. The labels in the boundary regions, which were masked in the unbleached vesicles, now contribute with the same weight as those far away from BR. A different order parameter in the boundary region should therefore lead to a change in the overall order parameter upon removal of the acceptor. The open symbols of Figure 5 show, however, that S does not change upon bleaching, except possibly at the highest BR/DMPC ratio. Due to the complexity of the problem, the analysis of our fluorescence data was based on the assumption of a single order parameter and viscosity. The above discussion shows that this assumption was justified. The conclusion from the data of Figure 5 is that the effect of BR on the order of the lipid phase has a range of at least 45 Å (R_0) and is probably homogeneous throughout the bilayer. A similar conclusion has been reached previously (Favre et al., 1979; Seelig & Seelig, 1978) by using different methods. The present results are in conflict with the recent suggestion of an exponential decay of the order parameter from the protein surface with a coherence length of about 15 Å (Jähnig, 1981).

The data for the microviscosity, η, calculated from the model-independent initial slope, show no dependence on the BR/DMPC ratio, for both unbleached and bleached vesicles. For the calculation of the initial slope, it is necessary to have an instrument with a good time resolution and an extremely stable lamp. A slight change in the pulse shape, especially at the rising edge, may have a drastic effect on the fast components of $r(t)$, and on r_0. As the time resolution of our instrument is ~0.2 ns, and as the lamp pulse is very stable, the initial slope can be calculated with good accuracy. The relative errors in η reflect the uncertainty in the initial slope. The standard deviations for $\bar{\phi}_{der}$ (~14%) are somewhat larger than for $\bar{\phi}_{int}$ (~8%); if ϕ_1 is a little too short, ϕ_2 will be a little too long and the amplitude R too large. In the products of eq 12, $R\phi_1$ and $(1 - R)\phi_2$, this error is compensated to some extent, whereas in the ratios of eq 13 it is amplified. The viscosities, η_{int}, calculated from the cone model are larger than the viscosities from the initial slope, because for a double-exponential decay the area under the decay curve $\bar{\phi}_{int}$ is always larger than $\bar{\phi}_{der}$. A single-exponential analysis, such as the approximation for the cone model (Kinosita et al., 1977), yields a correlation time, which is somewhere between $\bar{\phi}_{der}$ and $\bar{\phi}_{int}$, but the χ_ν^2 value is usually not acceptable. Moreover, the initial slope of the cone model approximation is not correct for the whole range of cone angles, including the isotropic case, $r_\infty = 0$ (compare eq 14 and 15 with $\bar{\phi}_{int} = \bar{\phi}_{der}$).

The increase of η_{int} with increasing BR/DMPC ratio calculated according to the cone model for bleached vesicles is not easily understood. It might be due to the unrealistic distribution function of this model (step function). As η_{int} was calculated from the area under the decay curve, its increase may arise from the order parameter of higher rank, $\langle P_4 \rangle$, $\langle P_6 \rangle$, etc., describing the real distribution function. Zannoni et al. (1983) derived a model for the anisotropy decay of DPH-like probes in macroscopically isotropic systems, such as vesicle suspensions. The anisotropy decay in their model is given by a sum of three exponentials and a constant term, where the correlation times and the preexponential factors are functions of $\langle P_2 \rangle$ ($\equiv S$) and $\langle P_4 \rangle$ [see eq 4.85 of Zannoni et al. (1983)]. According to this model, the area under the decay curve is therefore a function not only of $\langle P_2 \rangle$ and D_{int} (eq 14) but also of $\langle P_4 \rangle$. A disadvantage of their model is that, since the three correlation times are not given explicitly, it is not possible to calculate their parameters without making assumptions about the distribution function (Zannoni et al., 1983).

We note from Figures 5 and 6 that the results for S and η for the bleached vesicles are only significantly different from those of the unbleached vesicles at the highest BR/DMPC ratio (1/52). There is evidence from measurements of the rotational diffusion of BR that at this high ratio some BR aggregation occurs, which may explain the deviation (Cherry & Godfrey, 1981). If we disregard the results at BR/DMPC = 1/52, we may conclude from Figure 6 that the viscosity is approximately independent of the BR/DMPC ratio. When the data are evaluated on the basis of the initial slope, we find an average value of 0.144 P. With the cone model, the average value is twice as high, 0.292 P.

It is of considerable interest to compare these values for the viscosity from time-dependent fluorescence depolarization with those obtained from steady-state measurements using the standard microviscosity recipe (Shinitzky & Barenholz, 1978). In Table II, we have tabulated the viscosity values at 35 °C evaluated with various methods for the bleached vesicles. We left out the unbleached vesicles, because the complications of energy transfer were not taken into account in the microviscosity evaluation and an unfair comparison would result. The column labeled η_{MV} gives the microviscosity values evaluated from the steady-state anisotropy $\bar{r}$ by using the DPH lifetimes measured in these vesicles at 35 °C. It is apparent that already for the pure lipid vesicles a large discrepancy exists with the time-dependent result (η_{der}). This discrepancy increases when more and more BR is incorporated. For vesicles 6b, the discrepancy amounts to a factor of 10. As discussed in detail previously (Heyn, 1979; Heyn et al., 1981a), this failure of the microviscosity concept is mainly due to the assumption of unrestricted isotropic rotation corresponding to $r_\infty = 0$. This assumption is obviously wrong. An approximate correction for this neglect of r_∞ was recently suggested (Heyn et al., 1981a). The column labeled η_{cor} gives these corrected values. As expected, the correction goes into the right direction: the values are still much higher, however, than those obtained from the initial slope of $r(t)$. Since this correction requires a knowledge of r_∞, which is only available from time-dependent measurements, it does not offer a practical method for the estimation of η from steady-state measurements. In the last column of Table II, a comparison is made with the viscosity as determined from the rotational motion of BR in BR–DMPC

vesicles which were prepared in exactly the same way as described in this paper (Cherry & Godfrey, 1981). At 35 °C, a value of 3.7 ± 1.3 P is found, roughly independent of the protein to lipid ratio. The large discrepancy with the η_{der} values of the second to the last column, which are also approximately independent of this ratio, is apparent. This discrepancy was already noted before (Heyn et al., 1981a); however, at that time the viscosity values from the steady-state fluorescence depolarization measurements were not corrected for the effect of energy transfer, resulting in a much smaller discrepancy. There is at present no reason to question the Saffman–Delbrück theory on whose basis the viscosity η_{BR} was calculated. It seems more likely that these large differences are related to the size of the probe molecules.

Our values for S and η can now be compared with data from the literature obtained from time-dependent fluorescence anisotropy measurements on comparable vesicle systems. A similar large increase of the order parameter, S, of DPH at 35 °C from 0.30 to 0.69 upon addition of protein was observed for DMPC vesicles containing increasing amounts of cytochrome oxidase (maximal molar protein to lipid ratio 1/25) (Kinosita et al., 1981). The dependence of S on the protein to lipid ratio was linear with no sign of leveling off at the highest ratio. The higher order parameter in the presence of protein at 35 °C was interpreted as a reduction of the angular range of the rotational motion of the DPH labels within the boundary region of cytochrome oxidase. The strong energy transfer from DPH to the heme *a* of cytochrome oxidase (R_0 = 51 Å) leads to an exclusion of the labels in the neighborhood of the heme *a* from the observed ensemble average of the anisotropy decay. Due to a lack of knowledge on the size of the cytochrome oxidase molecule and the location of the heme group, an exact interpretation of the data was difficult. The lifetimes of DPH at the protein surface were estimated to be around 1 ns. The end values of the anisotropy decay were reached after 15–20 ns. Nevertheless, it was concluded that a significant amount of DPH at the protein surface will contribute to the observed anisotropy. At 35 °C, the wobbling diffusion constant, D_{int}, was not affected by the presence of cytochrome oxidase. Qualitatively, the same result was obtained for DPH in microsomal membranes from bovine adrenal cortex and its extracted lipid liposomes (Gallay et al., 1982). The order parameter of the protein-free liposomes at 40 °C was found to be 0.40, whereas in the microsomes at 39 °C it was 0.50. Again the wobbling diffusion constant, D_{int}, was unaffected by the proteins.

Differential polarized phase fluorometry with DPH in DMPC vesicles containing human apolipoprotein A-II also yields an increase in S upon addition of protein over a large range in temperatures above the phase transition temperature of DMPC (Mantulin et al., 1981). The use of the fluorescent acyl chain analogue *trans*-parinaric acid for the measurement of the effect of M-13 bacteriophage coat protein (CP) on the liquid-crystalline phase of DMPC leads to somewhat higher order parameters (S = 0.39 for pure DMPC at 39 °C) but to a similar increase upon addition of proteins (S = 0.57 for CP/DMPC = 1/30 at 39 °C) (Wolber & Hudson, 1982).

The articles cited above seem to suggest that membrane proteins always lead to an increase of the DPH order parameter. This is not the case, however. Recent measurements with cytochrome P-450 at 35 °C show that P-450 has no effect on the order of DPH in DMPC vesicles but lowers the order by about 30% in vesicles containing a mixture of phosphatidylcholine, phosphatidylserine, and phosphatidylethanolamine (B. Kunz et al., unpublished results). In this same lipid mixture, cytochrome P-450 reductase even leads to an order parameter of zero (B. Kunz et al., unpublished results).

Microviscosity values for various biological membranes, obtained from fluorescence anisotropy decay measurements, are in the range of 0.3–0.9 P (Kinosita et al., 1981; Glatz, 1978). Our present viscosity values derived from the initial slope (average 0.144 P) and from the cone model (average 0.292 P) fall in the same range. A recent evaluation of the NMR correlation times of deuterated lipids in sarcoplasmic reticulum vesicles in terms of microviscosity also yields low values ranging from 0.1 to 0.5 P (Seelig et al., 1981).

Registry No. DMPC, 13699-48-4; DPH, 1720-32-7; retinal, 116-31-4.

References

Badea, M. G., & Brand, L. (1979) *Methods Enzymol. 61*, 378–425.

Bevington, P. R. (1969) *Data Reduction and Error Analysis for the Physical Sciences*, McGraw-Hill, New York.

Cehelnik, E. D., Cundall, R. B., Lockwood, J. R., & Palmer, T. F. (1974) *J. Chem. Soc., Faraday Trans. 2 70*, 244–252.

Chen, L. A., Dale, R. E., Roth, S., & Brand, L. (1977) *J. Biol. Chem. 252*, 2163–2169.

Cherry, R. J., & Godfrey, R. E. (1981) *Biophys. J. 36*, 257–276.

Cherry, R. J., Müller, U., Henderson, R., & Heyn, M. P. (1978) *J. Mol. Biol. 121*, 283–298.

Dale, R. E., Chen, L. A., & Brand, L. (1977) *J. Biol. Chem. 252*, 7500–7510.

Dencher, N. A., Kohl, K.-D., & Heyn, M. P. (1983) *Biochemistry 22*, 1323–1334.

Favre, E., Baroin, A., Bienvenue, A., & Devaux, P. F. (1979) *Biochemistry 18*, 1156–1162.

Gallay, J., Vincent, M., & Alfsen, A. (1982) *J. Biol. Chem. 257*, 4038–4041.

Glatz, P. (1978) *Anal. Biochem. 87*, 187–194.

Grinvald, A. (1976) *Anal. Biochem. 75*, 260–280.

Grinvald, A., & Steinberg, I. Z. (1974) *Anal. Biochem. 59*, 583–598.

Heyn, M. P. (1979) *FEBS Lett. 108*, 359–364.

Heyn, M. P., & Dencher, N. A. (1982) *Methods Enzymol. 88*, 31–34.

Heyn, M. P., Cherry, R. J., & Dencher, N. A. (1981a) *Biochemistry 20*, 840–849.

Heyn, M. P., Blume, A., Rehorek, M., & Dencher, N. A. (1981b) *Biochemistry 20*, 7109–7115.

Heyn, M. P., Dencher, N. A., & Rehorek, M. (1983) in *Structure and Function of Membrane Proteins* (Quagliariello, E., & Palmieri, F., Eds.) pp 23–32, Elsevier, Amsterdam.

Jähnig, F. (1979) *Proc. Natl. Acad. Sci. U.S.A. 76*, 6361–6365.

Jähnig, F. (1981) *Biophys. J. 36*, 329–357.

Jost, P. C., & Griffith, O. H. (1982) *Lipid–Protein Interactions*, Vol. 1 and 2, Wiley, New York.

Kawato, S., Kinosita, K., & Ikegami, A. (1977) *Biochemistry 16*, 2319–2324.

Kinosita, K., Jr., Kawato, S., & Ikegami, A. (1977) *Biophys. J. 20*, 289–306.

Kinosita, K., Jr., Kawato, S., Ikegami, A., Yoshida, S., & Orii, Y. (1981) *Biochim. Biophys. Acta 647*, 7–17.

Kinosita, K., Jr., Ikegami, A., & Kawato, S. (1982) *Biophys. J. 37*, 461–464.

Lakowicz, J. R., Prendergast, F. G., & Hogen, D. (1979) *Biochemistry 18*, 520–527.

Lipari, G., & Szabo, A. (1980) *Biophys. J. 30*, 489–506.

Mantulin, W. W., Massey, J. B., Gotto, A. M., Jr., & Pownall, H. J. (1981) *J. Biol. Chem. 256*, 10815–10819.
Rehorek, M., Dencher, N. A., & Heyn, M. P. (1983) *Biophys. J. 43*, 39–45.
Seelig, A., & Seelig, J. (1978) *Hoppe-Seyler's Z. Physiol. Chem. 359*, 1747–1756.
Seelig, J., Tamm, L., Hymel, L., & Fleischer, S. (1981) *Biochemistry 20*, 3922–3932.
Seiff, F., Wallat, I., Ermann, P., & Heyn, M. P. (1985) *Proc. Natl. Acad. Sci. U.S.A. 82*, 3227–3231.
Shinitzky, M., & Barenholz, Y. (1978) *Biochim. Biophys. Acta 515*, 367–394.
Wahl, Ph. (1975) in *Biochemical Fluorescence: Concepts* (Chen, R. F., & Edelhoch, H., Eds.) pp 1–41, Marcel Dekker, New York.
Wahl, Ph. (1979) *Biophys. Chem. 10*, 91–104.
Wolber, P. K., & Hudson, B. S. (1982) *Biophys. J. 37*, 253–262.
Zannoni, C., Ariconi, A., & Cauatorta, P. (1983) *Chem. Phys. Lipids 32*, 179–250.

Simultaneous Observation of Order and Dynamics at Several Defined Positions in a Single Acyl Chain Using ^{2}H NMR of Single Acyl Chain Perdeuterated Phosphatidylcholines†

Michael R. Paddy‡ and F. W. Dahlquist*
Institute of Molecular Biology and Department of Chemistry, University of Oregon, Eugene, Oregon 97403
Edward A. Dratz and Alan J. Deese
Division of Natural Sciences and Chemistry Board of Studies, University of California, Santa Cruz, California 95064
Received December 19, 1984; Revised Manuscript Received May 3, 1985

ABSTRACT: Deuterium nuclear magnetic resonance (^{2}H NMR) spectra from aqueous dispersions of phosphatidylcholines in which perdeuterated palmitic acid is esterified at the *sn*-1 position have several very useful features. The powder spectra show six well-resolved 90° edges which correspond to the six positions closest to the methyl end of the acyl chain. The spectral overlap inherent in the multiple powder pattern line shape of these dispersions can be removed by using a "dePaking" procedure [Bloom, M., Davis, J. H., & Mackay, A. (1981) *Chem. Phys. Lett. 80*, 198–202] which calculates the spectra that would result if the lipid bilayers were oriented in the magnetic field. This procedure produces six well-resolved doublets whose NMR properties can be observed without interference from the resonances of other labeled positions. The presence of a single double bond in the *sn*-2 chain increases the order of the saturated 16:0 *sn*-1 chain at every position in the bilayer compared with a saturated *sn*-2 chain at the same reduced temperature. Surprisingly, addition of five more double bonds to the *sn*-2 chain only slightly reduces the order of the 16:0 *sn*-1 chain at many positions in the bilayer compared with the single double bond. Calculating oriented spectra from a spin–lattice (T_1) relaxation series of powder spectra allows one to obtain the T_1 relaxation times of six positions on the acyl chain simultaneously. As an example of the utility of these molecules, we demonstrate that the dependence of the spin–lattice (T_1) relaxation rate as a function of orientational order for two unsaturated phospholipids differs significantly from the corresponding fully saturated analogue. Interpreting this difference using current models of acyl chain dynamics suggests that the bilayers containing either of the two unsaturated phospholipids are significantly more deformable than bilayers made from the fully saturated phospholipid.

Over the last several years, deuterium nuclear magnetic resonance (^{2}H NMR)[1] methods have become widely recognized as particularly effective probes of molecular motion in anisotropic biological systems. Determination of the orientational order parameter from ^{2}H NMR spectra can directly yield the average amplitude of motions which occur on a time scale of $\sim 10^{-6}$ s or faster. Determinations of ^{2}H NMR relaxation times reflect the rates of these motions and may allow calculation of the reorientational correlation times. In principal, then, it is possible to measure the amplitudes and rates of the molecular motion separately. Furthermore, since the

† This work was supported by grants from the National Institutes of Health (RO1EY400175, IF32E405607, and GM24792) and by a National Institutes of Health Training Grant (GM07759). F.W.D. is a recipient of an American Cancer Society Faculty Research Award.
* Address correspondence to this author at the Institute of Molecular Biology, University of Oregon.
‡ Present address: Department of Biochemistry and Biophysics, University of California, San Francisco, CA 94143.

[1] Abbreviations: ^{2}H NMR, deuterium nuclear magnetic resonance; T_1, spin–lattice relaxation time; (16:0)(16:0)PC, 1,2-dipalmitoyl-*sn*-glycero-3-phosphocholine; (16:0)(16:1)PC, 1-palmitoyl-2-palmitoleoyl-*sn*-glycero-3-phosphocholine; (16:0)(22:6)PC, 1-palmitoyl-2-docosahexaenoyl-*sn*-glycero-3-phosphocholine; (16:0)(18:1)PC, 1-palmitoyl-2-oleoyl-*sn*-glycero-3-phosphocholine; $1/T_{2e}$, rate of decay of the quadrupolar echo; θ, reduced temperature; BHT, butylated hydroxytoluene; TLC, thin-layer chromatography; GLC, gas–liquid chromatography; HEPES, *N*-(2-hydroxyethyl)piperazine-*N'*-2-ethanesulfonic acid.

0006-2960/85/0424-5988$01.50/0